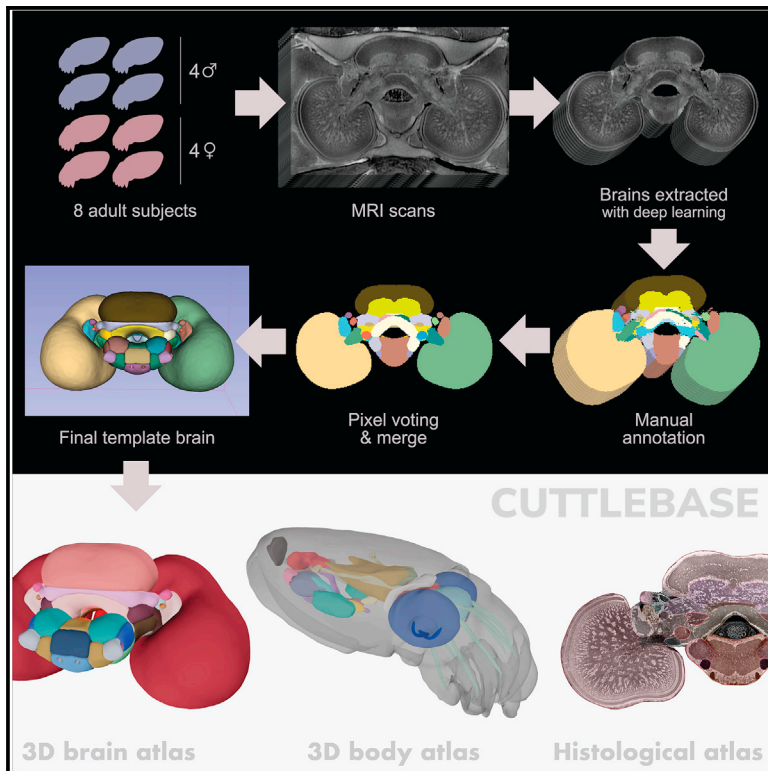


# Current Biology

## A brain atlas for the camouflaging dwarf cuttlefish, *Sepia bandensis*

### Graphical abstract



### Authors

Tessa G. Montague, Isabelle J. Rieth, Sabrina Gjerwold-Selleck, ..., Rebecca A. Ober, Jia Guo, Richard Axel

### Correspondence

tessa.montague@columbia.edu (T.G.M.), ra27@columbia.edu (R.A.)

### In brief

Cephalopods are masters of dynamic camouflage and complex social behaviors, and they exhibit learning and memory. Montague et al. generate a brain atlas for a promising model cephalopod species, the dwarf cuttlefish, using magnetic resonance imaging, deep learning, and histology. They host the data on a custom-built interactive website, Cuttlebase.

### Highlights

- A 3D cuttlefish brain atlas, generated from 8 brains using MRI and deep learning
- A histological brain atlas, in 3 planes, annotated with 32 brain lobes
- A 3D body atlas, annotated with 26 organs
- All tools hosted on a custom-built website, <https://www.cuttlebase.org/>

Report

# A brain atlas for the camouflaging dwarf cuttlefish, *Sepia bandensis*

Tessa G. Montague,<sup>1,2,5,\*</sup> Isabelle J. Rieth,<sup>1</sup> Sabrina Gjerswold-Selleck,<sup>1</sup> Daniella Garcia-Rosales,<sup>1</sup> Sukanya Aneja,<sup>3</sup> Dana Elkis,<sup>3</sup> Nanyan Zhu,<sup>1</sup> Sabrina Kentis,<sup>1</sup> Frederick A. Rubino,<sup>4</sup> Adriana Nemes,<sup>1</sup> Katherine Wang,<sup>1</sup> Luke A. Hammond,<sup>1</sup> Roselis Emiliano,<sup>1</sup> Rebecca A. Ober,<sup>1</sup> Jia Guo,<sup>1</sup> and Richard Axel<sup>1,2,\*</sup>

<sup>1</sup>The Mortimer B. Zuckerman Mind Brain Behavior Institute, Department of Neuroscience, Columbia University, New York, NY 10027, USA

<sup>2</sup>Howard Hughes Medical Institute, Columbia University, New York, NY 10027, USA

<sup>3</sup>Interactive Telecommunications Program, New York University, New York, NY 10003, USA

<sup>4</sup>Department of Cell Biology, NYU Grossman School of Medicine, New York, NY 10016, USA

<sup>5</sup>Lead contact

\*Correspondence: [tessa.montague@columbia.edu](mailto:tessa.montague@columbia.edu) (T.G.M.), [ra27@columbia.edu](mailto:ra27@columbia.edu) (R.A.)

<https://doi.org/10.1016/j.cub.2023.06.007>

## SUMMARY

The coleoid cephalopods (cuttlefish, octopus, and squid) are a group of soft-bodied marine mollusks that exhibit an array of interesting biological phenomena, including dynamic camouflage, complex social behaviors, prehensile regenerating arms, and large brains capable of learning, memory, and problem-solving.<sup>1–10</sup> The dwarf cuttlefish, *Sepia bandensis*, is a promising model cephalopod species due to its small size, substantial egg production, short generation time, and dynamic social and camouflage behaviors.<sup>11</sup> Cuttlefish dynamically camouflage to their surroundings by changing the color, pattern, and texture of their skin. Camouflage is optically driven and is achieved by expanding and contracting hundreds of thousands of pigment-filled saccules (chromatophores) in the skin, which are controlled by motor neurons emanating from the brain. We generated a dwarf cuttlefish brain atlas using magnetic resonance imaging (MRI), deep learning, and histology, and we built an interactive web tool (<https://www.cuttlebase.org/>) to host the data. Guided by observations in other cephalopods,<sup>12–20</sup> we identified 32 brain lobes, including two large optic lobes (75% the total volume of the brain), chromatophore lobes whose motor neurons directly innervate the chromatophores of the color-changing skin, and a vertical lobe that has been implicated in learning and memory. The brain largely conforms to the anatomy observed in other *Sepia* species and provides a valuable tool for exploring the neural basis of behavior in the experimentally facile dwarf cuttlefish.

## RESULTS

### An MRI-based 3D brain atlas of the dwarf cuttlefish

The dwarf cuttlefish, *Sepia bandensis*, is a small tropical species from the Indo-Pacific (Figure 1A) that exhibits a rich repertoire of behaviors. The skin of the dwarf cuttlefish is covered in hundreds of thousands of chromatophores (pigment-filled saccules surrounded by radial muscles) whose expansion states are controlled by motor neurons projecting from the brain.<sup>21</sup> During camouflage (Figure 1B), conspecific communication (Figures 1C and 1D), and deimatic behavior, dwarf cuttlefish dynamically alter the color, pattern, and texture of their skin using chromatophores and subcutaneous papillae. This process is driven by visual circuits in the brain and is therefore extremely rapid, occurring in milliseconds.<sup>22,23</sup> Thus, the skin patterning of cuttlefish reflects both the organism's perception of the external world and its internal state.

The dwarf cuttlefish brain is located posterior and medial to the eyes and is encased on the posterior side by cranial cartilage (Figure 1E). We performed *ex vivo* magnetic resonance imaging (MRI) of the brains of 8 adult dwarf cuttlefish (4 males, 4 females)

at 50  $\mu\text{m}$  isotropic resolution and then combined manual segmentation with deep learning techniques to extract each brain from its surrounding tissue (STAR Methods; Figure S1). Using 6 independent annotators, we segmented the brain lobes using prior neuroanatomical descriptions as a guide<sup>12,18,19</sup> and performed pixel-voting to generate consensus boundaries. The final segmentations of the 8 brains were similar in total volume, as well as in absolute (Table S1) and relative (Table S2) lobe volumes. We detected no significant size differences between the male and female brains (Tables S1 and S2). We therefore co-registered the 8 brains to create a merged, annotated template brain (Figure 1F; Table S3).

The *ex vivo* dwarf cuttlefish brain is 94% the volume of the *ex vivo* mouse brain (Table S3; STAR Methods). The cuttlefish brain surrounds the esophagus and can be coarsely divided into a supraesophageal mass and a subesophageal mass<sup>24,25</sup> that we further divided into 32 discrete lobes (Table 1). This value is in accord with previous anatomical studies in other species, but it remains possible that the annotated lobes can be subdivided further. The functions of most cephalopod brain lobes are unknown, but some have been assigned function through

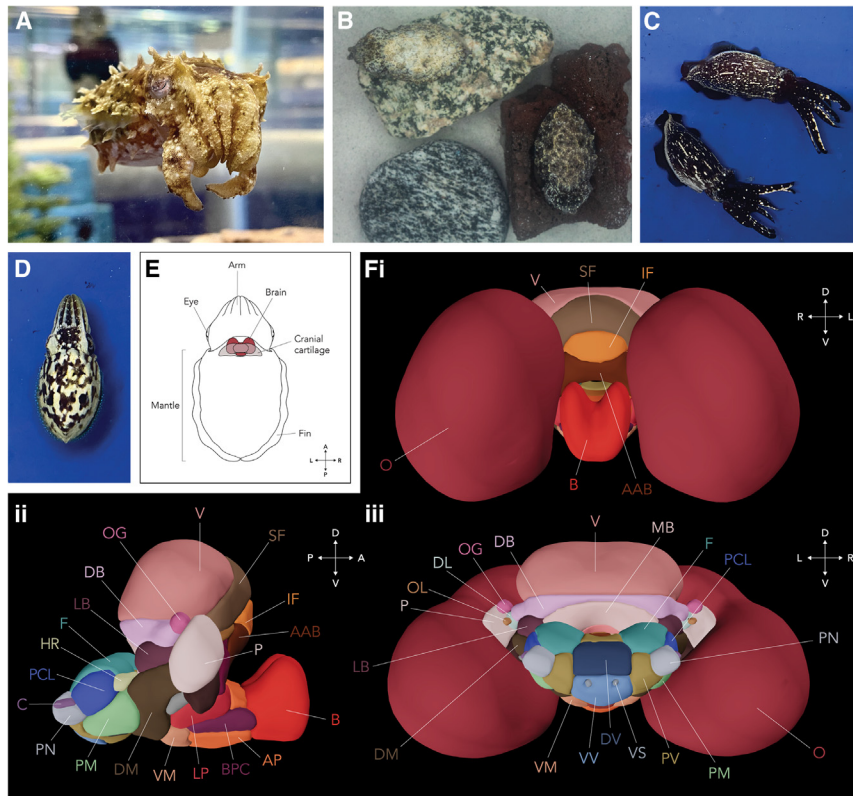


**Figure 1. 3D brain atlas for the dwarf cuttlefish, *Sepia bandensis***

(A) Adult dwarf cuttlefish (~8 cm in total body length).

(B) Cuttlefish camouflage to their surroundings by changing the color, pattern, and texture of their skin.

(C) The innate skin pattern and posture adopted by male dwarf cuttlefish during aggressive interactions.

(D) An innate skin pattern frequently adopted by dwarf cuttlefish in the presence of conspecifics.

(E) Anatomy of a cuttlefish. The brain is encased on its posterior side by rigid cartilage.

(F) 3D template brain, based on magnetic resonance imaging (MRI) of 8 brains (4 males, 4 females) and manual annotations of 32 brain lobes and 12 nerve tracts. For abbreviations, see [Table 1](#). (i) Anterior view, (ii) right view (shown without the optic lobes), and (iii) posterior view. See also [Figure S1](#) and [Tables S1–S4](#).

chromatophore lobes are thought to coordinate skin patterns between the head, arms, and body.<sup>14</sup>

The posterior region of the subesophageal mass (the posterior subesophageal mass, PSM) projects through an opening in the cranial cartilage ([Figure 3B](#)). Structures in this region control motor actions in the more posterior aspect of the cuttlefish. For instance, the posterior chromatophore lobes (PCL) control the chromatophores of the mantle ([Figures 1Fii and 1Fiii](#)), the fin lobes (F) control movement of the fins ([Figures 1Fii and 1Fiii](#)), and the palliovisceral lobe (PV) controls escape movements and inking ([Figure 1Fiii](#)), which are mediated by the funnel.<sup>18</sup> These attributed functions reflect observations in other cephalopod species.

lesion experiments<sup>26–31</sup> and electrophysiological studies.<sup>18,32–42</sup> Moreover, coarse connectivity has been elucidated by neural tracing techniques<sup>12–17</sup> and probabilistic tractography.<sup>19,43</sup>

We have related the existing knowledge on the function and connectivity of cephalopod lobes to the *Sepia bandensis* anatomy presented here. The largest brain lobes, the optic lobes (O), comprise 75% of the total volume of the brain ([Table S3](#)), receive direct projections from the retina, and are engaged in visual processing<sup>13</sup> ([Figures 1Fi and 1Fiii](#)). One relevant projection of the optic lobe is the lateral basal lobe (LB), an intermediate station in the camouflage pathway<sup>12,13,18,20</sup> that may use processed visual information from the optic lobes to compute the most appropriate skin pattern components for camouflage. The vertical lobe complex lies on the dorsal side of the supraesophageal mass ([Figure 1F](#)). This complex is considered to be the learning and memory center of the brain<sup>45</sup> and may facilitate short-term,<sup>46</sup> spatial,<sup>31</sup> and visual<sup>44</sup> learning in cephalopods, including working<sup>47</sup> and episodic-like memory.<sup>48</sup> The vertical lobe (V) is directly underneath the dorsal cranial cartilage—an ideal structure for anchoring an electrode or GRIN lens for neural recordings<sup>49</sup> ([Figure 3B](#)).

The subesophageal mass comprises multiple structures that elicit motor actions. There is a rough mapping of lobe position in the brain to motor target in the body. For instance, the lobes in the anterior portion of the subesophageal mass control movements of structures in the anterior portion of the cuttlefish: the brachial lobe (B) controls the arms, the lateral pedal lobes (LP) control movements of the eyes ([Figure 1Fii](#)), and the anterior chromatophore lobes control the chromatophores of the head and arms.<sup>18</sup> Connections between the anterior and posterior

### A histological brain atlas for the dwarf cuttlefish

We complemented the anatomical description of the cuttlefish brain with histological examination of the entire brain to obtain cellular resolution. We sectioned the brain in the transverse, horizontal, and sagittal planes ([Figure 2A](#)) and stained the sections with Phalloidin, an F-actin peptide that labels axons, and NeuroTrace, a Nissl stain that labels neuronal cell bodies and glia. Our annotated 3D MRI datasets and prior neuroanatomical descriptions<sup>12,18,19</sup> were used to describe the histological organization of 32 brain lobes and 12 nerve tracts ([Figures 2B–2D](#)).

Phalloidin and NeuroTrace staining confirmed previously described organizational features of the cephalopod brain. Most lobes are discrete and bounded, a feature not uniformly observed in vertebrate brains: each lobe contains an outer perikaryal layer of cell bodies that surrounds a dense, inner neuropil ([Figures 2B–2D](#)).<sup>12</sup> Dwarf cuttlefish neuronal cell bodies range in diameter from ~5 μm (e.g., the vertical and optic lobes) to <80 μm in some motor areas (e.g., the fin and pedal lobes) ([Figures 2E–2G](#)).

Similar to other coleoid cephalopods, the *Sepia bandensis* optic lobe consists of two ordered outer layers, the inner and outer granular layers, apposing a zone of fibers ([Figure 2E](#)).<sup>13,20,50</sup>

**Table 1. The brain lobes of the dwarf cuttlefish, *Sepia bandensis***

Brain region	Abbreviation	Function
<b>Supraesophageal mass</b>		
Vertical lobe complex		learning and memory <sup>44</sup>
vertical lobe	V	
subvertical lobe	SV	
superior frontal lobe	SF	
inferior frontal lobe	IF	
posterior frontal lobe	PF	
Basal lobe complex		higher motor control <sup>18</sup>
anterior anterior basal lobe	AAB	movement of head, arms, and eyes
anterior posterior basal lobe	APB	
precommissural lobe	PC	
dorsal basal lobe	DB	
interbasal lobes	IB	movement of feeding tentacles
median basal lobe	MB	movement of mantle and funnel during swimming and breathing, protraction and retraction of head, movement of fins, movement of buccal mass, and expansion and contraction of chromatophores
lateral basal lobes	LB	control of chromatophores and papillae
<b>Subesophageal mass</b>		
Pedal lobe complex		intermediate and lower motor control of movement <sup>18</sup>
anterior pedal lobe	AP	movement of arms and tentacles
posterior pedal lobe	PP	movement of funnel, fins, and tentacles; head retraction
lateral pedal lobes	LP	movement of eyes
anterior dorsal chromatophore lobes	ADC	control of chromatophores and papillae on the head and arms
anterior ventral chromatophore lobes	AVC	control of chromatophores and papillae on the head and arms
Magnocellular lobe complex		giant fiber response (breathing) <sup>18</sup>
dorsal magnocellular lobes	DM	
ventral magnocellular lobes	VM	
posterior magnocellular lobes	PM	
Palliovisceral lobe complex		lower motor control of locomotion <sup>18</sup>
palliovisceral lobe	PV	control of escape movements and ink ejection
lateral ventral palliovisceral lobes	LVP	
fin lobes	F	movement of fins
posterior chromatophore lobes	PCL	control of chromatophores and papillae on mantle, fin, and visceral mass
dorsal vasomotor lobe	DV	
ventral vasomotor lobe	VV	
Brachial lobe complex		motor control of arms and feeding <sup>18</sup>
brachial lobe	B	intermediate motor control of arms
superior buccal lobe	SB	biting movements of the buccal mass (not featured in 3D brain atlas)
inferior buccal lobe	IB	biting movements of the buccal mass (not featured in 3D or histological atlas)
<b>Periesophageal mass</b>		
Optic tract complex		
optic lobes	O	visual processing <sup>18</sup>
peduncle lobes	P	visuo-motor control <sup>30</sup>
dorsolateral lobes	DL	

(Continued on next page)

**Table 1. Continued**

Brain region	Abbreviation	Function
optic glands	OG	neurosecretory center <sup>30</sup>
olfactory lobes	OL	unclear function <sup>16</sup>
<b>Nerve fibers</b>		
anterior magnocellular commissure	AMC	
brachio-palliovisceral connectives	BPC	
collar nerves	C	innervation of the collar muscles and valves of the mantle <sup>12</sup>
head retractor nerves	HR	innervation of the muscles that connect the head to the mantle <sup>12</sup>
lateral basal to posterior chromatophore lobe tracts	LBPC	
optic to anterior basal lobe tracts	OAB	
optic to dorsal magnocellular lobe tracts	ODM	
optic to vertical lobe tracts	OV	
pallial nerves	PN	innervation of the muscles and skin of the mantle and visceral mass <sup>12</sup>
subvertical to optic tracts	SOT	
ventral optic commissure	VOC	
visceral nerves	VS	innervation of retractor muscles of the head and funnel; ink sac; heart; main blood vessels; and digestive, excretory, and reproductive systems <sup>12</sup>

Because the cephalopod retina contains only photoreceptors, the outer layers of the optic lobe may function like the vertebrate retina and perform the initial stages of visual processing.<sup>50,51</sup> Beneath the outer layers, the cephalopod optic lobe features a novel neural organization: a central medulla that features cell “islands” (Figure 2F) connected in an elaborate tree-like structure.<sup>13,20,52</sup> Cell bodies near the cortex (the “branches”) appear to form columns (Figures 2B and 2C), which may reflect the presumed retinotopic order of the outer layers.<sup>13,20,53</sup>

Five pairs of nerves project from the cuttlefish brain that are easily distinguishable in histological slices and contain many of the brain’s major efferents. The largest nerves, the pallial nerves (PN), exit the posterior side of the brain and contain motor fibers that innervate the chromatophores and muscles of the mantle and fin (Figure 2B).<sup>12</sup> The motor neurons that originate in the posterior chromatophore lobe exit via the pallial nerve, pass through the stellate ganglion, and directly innervate the radial muscles of the chromatophores.<sup>54</sup> Severing a pallial nerve results in blanched skin, loss of the skin’s textural control, and a limp fin on the ipsilateral side of the body.<sup>55</sup> Closely apposed to the pallial nerves are the collar nerves (C), which innervate the collar muscles and valves of the mantle (Figure 2B).<sup>12</sup> The visceral nerves are positioned near the midline on the posterior side of the brain and innervate the heart, ink sac muscles, and digestive, reproductive, and excretory systems.<sup>12</sup> Finally, the head retractor nerves (HR), positioned ventral to the lateral basal lobes, innervate the muscles that connect the head to the mantle (Figure 2B).<sup>12</sup> When dwarf cuttlefish sense danger, they can retract their head inside their body using these muscles.

### Cuttlebase—a web tool for visualizing the cuttlefish brain

We built an interactive web tool, Cuttlebase, to maximize the utility of our brain atlas (Figure 3A). Cuttlebase features multiple tools for the dwarf cuttlefish, including the annotated histological sections of the brain in 3 planes (Figure 3A), the 3D brain model described above (Figure 3B), and a 3D model of an entire adult cuttlefish labeled with 26 organs, including the animal’s three hearts, gills, ink sac, beak, cuttlebone, and digestive system (Figure 3C). Furthermore, the 3D body model features the eight brachial nerves that innervate the cuttlefish’s arms, and the two pallial nerves, which exit the posterior aspect of the brain, circumscribe the digestive gland, and then pass through a hole in the mantle musculature to reach the stellate ganglion.<sup>56</sup> Cuttlebase is easy to use, with an array of features including responsive color-coded labels for each brain region; a dynamic scale bar; the ability to zoom, rotate, and screenshot the data; and synchronized graphics that denote the brain’s orientation (Figure 3B).

Cuttlebase was designed for both educational and research settings. For its use in education, we added features that increase accessibility, including (1) a landing page that introduces cuttlefish behavior, brain anatomy, evolution, and animal care; (2) an info page that shows the cuttlefish’s gross anatomy and the sectioning planes used in the histological atlas; (3) an option to show the 3D brain model in the context of the cuttlefish’s body; and (4) mouseover descriptions of the function of each brain lobe. For expert users, we included an array of more advanced features. First, we included a dynamic scale bar in the histology mode to help users measure distances within the

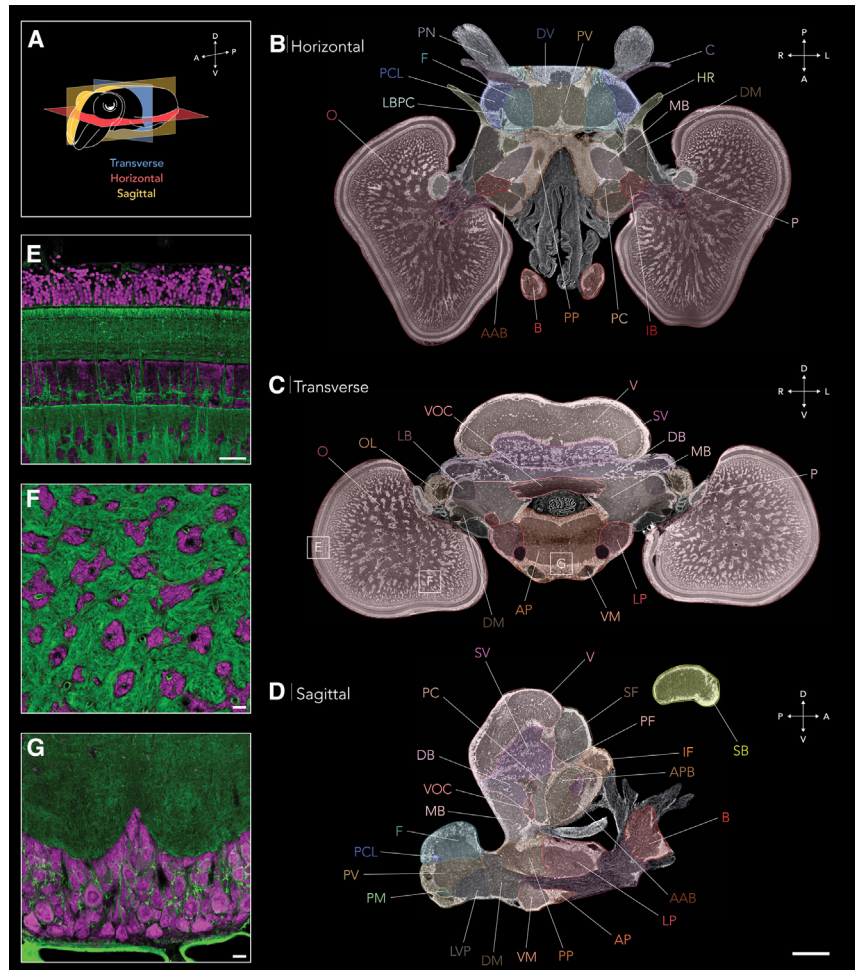


**Figure 2. Histological brain atlas for the dwarf cuttlefish**

(A) The dwarf cuttlefish brain was sectioned in the transverse, horizontal, and sagittal planes. (B–D) Representative histological slices of the cuttlefish brain stained with NeuroTrace (a Nissl stain that labels cell bodies) and annotated with 32 brain lobes and 12 nerve tracts. Scale bar, 1 mm. For abbreviations, see Table 1. Boxed areas in (C) show approximate locations of confocal images within the brain. (E–G) Confocal images of cuttlefish tissue stained with NeuroTrace (purple) and Phalloidin (an F-actin peptide that labels axons, green). (E) Optic lobe layered cortex. (F) Optic lobe medulla (G) Anterior pedal lobe. Confocal scale bars, 50  $\mu$ m.

extensively to understand behavior,<sup>8</sup> learning and memory,<sup>1</sup> and the neural control of skin patterning.<sup>4,23</sup> Qualitative comparison of our dataset with the neuroanatomy of the common cuttlefish<sup>18,57</sup> reveals substantial neuroanatomic resemblance despite the species' different sizes, behaviors, and habits.<sup>11,58</sup> *Sepia bandensis*, a small cuttlefish species that lives in Indo-Pacific coral reefs, assembles skin patterns with predominantly high-frequency components, likely reflecting the visual statistics of their tropical habitat. By contrast, *Sepia officinalis*, a medium-sized species that lives in the rocky waters of Europe, includes a repertoire of large, disruptive

patterns that resemble rocks.<sup>58</sup> During male social encounters, *Sepia officinalis* and *Sepia bandensis* exhibit a high-contrast, stereotyped aggression pattern that differs in the two species: *Sepia officinalis* create a zebra pattern,<sup>58</sup> whereas the *Sepia bandensis* aggression pattern is stippled (Figure 1C).<sup>11</sup> Such fine-scale differences are unlikely to be reflected at the coarse anatomic level, but may be more evident in the analysis of patterns of neural activity. The generation of cephalopod cell atlases<sup>59–62</sup> and their assignment to neuroanatomical atlases will help build a more comprehensive view of cephalopod brain organization.

## DISCUSSION

The 3D and histological brain atlases presented here serve as a useful resource for the investigation of the neural basis of cephalopod behavior. Users can employ Cuttlebase to guide electrode and GRIN lens insertion. Moreover, the histological atlas affords users the ability to identify experimentally targeted brain regions. The histological atlas can also be used to study spatially restricted gene expression and neural activity as defined by immediate early gene expression.

This atlas also functions as a resource for comparative neuroanatomical analyses. Little is currently known about the biology of the dwarf cuttlefish (*Sepia bandensis*), whereas the common cuttlefish (*Sepia officinalis*) has been studied

Quantitative comparison of the *Sepia bandensis* brain with the annotated brains of two cephalopod species of similar body sizes (mourning cuttlefish, *Sepia plangon*,<sup>43</sup> and juvenile bigfin reef squid, *Sepioteuthis lessoniana*<sup>19</sup>) reveals coarse similarity in relative lobe volumes in all three species (Table S4). Some volumetric differences, such as the smaller vertical lobe of *Sepioteuthis lessoniana*, could reflect underlying biological differences. However, larger sample sizes and brain lobe boundary consensus are needed before reliable quantitative cross-species volume comparisons can be made.

This atlas also permits neuroanatomical comparisons across phyla. Despite ~600 million years of separation

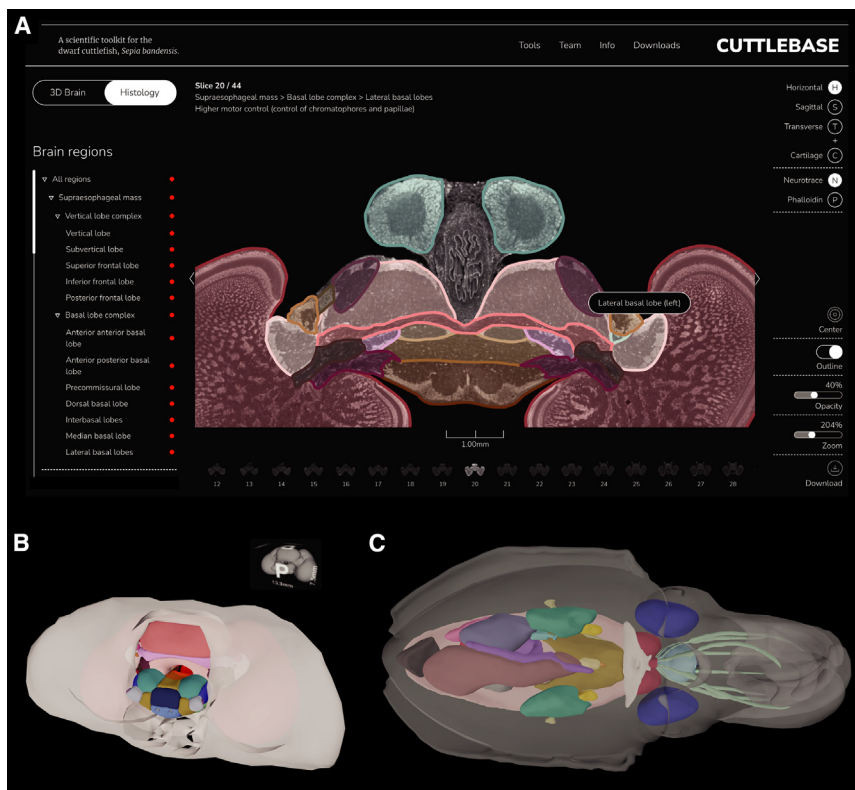


**Figure 3. Cuttlebase is a scientific toolkit for the dwarf cuttlefish**

(A) Cuttlebase (<https://www.cuttlebase.org/>) hosts multiple dwarf cuttlefish tools including an interactive histological brain atlas, which features color-coded and responsive labels; a dynamic scale bar; and the ability to screenshot, zoom, and rotate the data.

(B) The 3D brain atlas can be visualized with the cranial cartilage and features a synchronized graphic that denotes the brain's orientation.

(C) Cuttlebase also features a body atlas, labeled with 26 organs and tissues.

between cuttlefish and fruit flies,<sup>63</sup> the brains of these species share coarse organizational features. The esophagus runs through the center of the brain, two large optic lobes flank the central brain mass, and the learning and memory centers—the mushroom body in *Drosophila* and the vertical lobe in cuttlefish—lie on the dorsal side of the brain. Furthermore, the two outer layers of the cuttlefish optic lobe may share properties with the lamina and medulla of the dipteran visual system.<sup>64</sup> Interestingly, recent single-cell gene expression profiling of a developing octopus brain has revealed molecular resemblances between the Kenyon cells of the *Drosophila* mushroom body and the vertical lobe cells of the octopus brain.<sup>61</sup> The combination of anatomical, cellular, and molecular maps of the cephalopod brain should provide insight into how these invertebrate mollusks evolved their complex cognitive abilities and behaviors.

In summary, Cuttlebase was designed to aid the investigation of cuttlefish biology and now renders *Sepia bandensis* a more facile system for the study of the neural control of behavior.

## STAR★METHODS

Detailed methods are provided in the online version of this paper and include the following:

- KEY RESOURCES TABLE
- RESOURCE AVAILABILITY
  - Lead contact
  - Materials availability
  - Data and code availability

## ● EXPERIMENTAL MODEL AND SUBJECT DETAILS

- Ethics statement
- Cuttlefish husbandry

## ● METHOD DETAILS

- 3D brain atlas
- Histological atlas
- Whole body atlas
- Cuttlebase

## ● QUANTIFICATION AND STATISTICAL ANALYSIS

## SUPPLEMENTAL INFORMATION

Supplemental information can be found online at <https://doi.org/10.1016/j.cub.2023.06.007>.

## ACKNOWLEDGMENTS

We wish to thank Connor Gibbons, Sonia Thomas, Telicia Lewis, Sarah Wilson, and Josh Barber for cuttlefish care; the Zuckerman Institute Cellular Imaging platform for instrument use and technical support; Lokke Highstein for IT support; Lucas Pozzo-Miller, Judit Pungor, Barbara Noro, Andrés Bendesky, Bret Grasse, Josh Barber, and Denise Piscopo for Cuttlebase testing; and Carrie Albertin for valuable discussions. This project was funded by a Zuckerman Institute MRI Seed Grant (T.G.M. and R.A.), the Howard Hughes Medical Institute Hanna H. Gray Fellowship (T.G.M.), the Zuckerman Institute BRAINYAC Program (R.E.), and the Howard Hughes Medical Institute (R.A.).

## AUTHOR CONTRIBUTIONS

T.G.M., R.A.O., and J.G. conceived the project. T.G.M., I.J.R., S.G.-S., and J.G. performed MRI experiments. T.G.M. performed histology experiments. S.G.-S. conducted MRI data processing steps, with input from N.Z. and J.G. MRI data were annotated by I.J.R., T.G.M., D.G.-R., S.K., F.A.R., A.N., K.W.,

and R.E. Histology data were annotated by I.J.R. and T.G.M. L.A.H. developed the BrainJ software. D.E. designed and S.A. developed the Cuttlebase website. J.G. and R.A. provided supervision. T.G.M. wrote the original draft of the manuscript. T.G.M. and R.A. reviewed and edited the manuscript. T.G.M. and R.A. acquired funding for the project.

#### DECLARATION OF INTERESTS

The authors declare no competing interests.

#### INCLUSION AND DIVERSITY

We support inclusive, diverse, and equitable conduct of research. One or more of the authors of this paper self-identifies as an underrepresented ethnic minority in their field of research or within their geographical location. One or more of the authors of this paper self-identifies as a member of the LGBTQIA+ community. One or more of the authors of this paper received support from a program designed to increase minority representation in their field of research.

Received: April 11, 2023

Revised: May 30, 2023

Accepted: June 1, 2023

Published: June 20, 2023

#### REFERENCES

1. Turchetti-Maia, A., Shomrat, T., and Hochner, B. (2019). The vertical lobe of cephalopods: a brain structure ideal for exploring the mechanisms of complex forms of learning and memory. In *The Oxford Handbook of Invertebrate Neurobiology*, J.H. Byrne., ed. (Oxford University Press), pp. 559–574.
2. Fiorito, G., von Planta, C., and Scotto, P. (1990). Problem solving ability of *Octopus vulgaris* Lamarck (Mollusca, Cephalopoda). *Behav. Neural. Biol.* *53*, 217–230.
3. Richter, J.N., Hochner, B., and Kuba, M.J. (2016). Pull or push? Octopuses solve a puzzle problem. *PLoS One* *11*, e0152048.
4. Reiter, S., Hülshunk, P., Woo, T., Lauterbach, M.A., Eberle, J.S., Akay, L.A., Longo, A., Meier-Credo, J., Kretschmer, F., Langer, J.D., et al. (2018). Elucidating the control and development of skin patterning in cuttlefish. *Nature* *562*, 361–366.
5. Schnell, A.K., and Clayton, N.S. (2019). Cephalopod cognition. *Curr. Biol.* *29*, R726–R732.
6. Imperadore, P., and Fiorito, G. (2018). Cephalopod tissue regeneration: consolidating over a century of knowledge. *Front. Physiol.* *9*, 593.
7. Amodio, P., Boeckle, M., Schnell, A.K., Ostojic, L., Fiorito, G., and Clayton, N.S. (2019). Grow smart and die young: why did cephalopods evolve intelligence. *Trends Ecol. Evol.* *34*, 45–56.
8. Hanlon, R.T., and Messenger, J.B. (2018). *Cephalopod Behaviour* (Cambridge University Press).
9. Osorio, D., Ménager, F., Tyler, C.W., and Darmaillacq, A.S. (2022). Multi-level control of adaptive camouflage by European cuttlefish. *Curr. Biol.* *32*, 2556–2562.e2.
10. How, M.J., Norman, M.D., Finn, J., Chung, W.S., and Marshall, N.J. (2017). Dynamic skin patterns in cephalopods. *Front. Physiol.* *8*, 393.
11. Montague, T.G., Rieth, I.J., and Axel, R. (2021). Embryonic development of the camouflaging dwarf cuttlefish, *Sepia bandensis*. *Dev. Dyn.* *250*, 1688–1703.
12. Young, J.Z. (1971). *The Anatomy of the Nervous System of Octopus Vulgaris* (Oxford University Press).
13. Young, J.Z. (1974). The central nervous system of *Loligo*. I. The optic lobe. *Philos. Trans. R. Soc. Lond. B Biol. Sci.* *267*, 263–302.
14. Young, J.Z. (1976). The nervous system of *Loligo*. II. Suboesophageal centres. *Philos. Trans. R. Soc. Lond. B Biol. Sci.* *274*, 101–167.
15. Young, J.Z. (1977). The nervous system of *Loligo*, III. Higher motor centres: the basal supraoesophageal lobes. *Philos. Trans. R. Soc. Lond. B Biol. Sci.* *276*, 351–398.
16. Young, J.Z. (1979). The nervous system of *Loligo*. V. The vertical lobe complex. *Philos. Trans. R. Soc. Lond. B Biol. Sci.* *285*, 311–354.
17. Messenger, J.B. (1979). The nervous system of *Loligo* IV. The peduncle and olfactory lobes. *Philos. Trans. R. Soc. Lond. B Biol. Sci.* *285*, 275–309.
18. Boycott, B.B. (1961). The functional organization of the brain of the cuttlefish *Sepia officinalis*. *Proc. Royal Soc. B* *153*, 503–534.
19. Chung, W.S., Kurniawan, N.D., and Marshall, N.J. (2020). Toward an MRI-based mesoscale connectome of the squid brain. *iScience* *23*, 100816.
20. Young, J.Z. (1962). The optic lobes of *Octopus vulgaris*. *Philos. Trans. R. Soc. Lond. B Biol. Sci.* *245*, 19–58.
21. Messenger, J.B. (2001). Cephalopod chromatophores: neurobiology and natural history. *Biol. Rev. Camb. Philos. Soc.* *76*, 473–528.
22. Hill, A.V., and Solandt, D.Y. (1935). Myograms from the chromatophores of *Sepia*. *J. Physiol. Lond.* *83*, 13P–14P.
23. Hanlon, R. (2007). Cephalopod dynamic camouflage. *Curr. Biol.* *17*, R400–R404.
24. Dietl, M.J. (1878). Untersuchungen über die Organisation des Gehirns wirbelloser Thiere (Cephalopoden, Tethys). *Sitzungsberichte der Akademie der Wissenschaften in Wien* *77*, 481–533.
25. Hillig, R. (1912). Das Nervensystem von *Sepia officinalis*. *L. Z. wiss. Zool.* *101*, 736–800.
26. Wells, M.J., and Young, J.Z. (1975). The subfrontal lobe and touch learning in the octopus. *Brain Res.* *92*, 103–121.
27. Boycott, B.B., and Young, J.Z. (1957). Effects of interference with the vertical lobe on visual discriminations in *Octopus vulgaris* Lamarck. *Proc. R. Soc. Lond. B Biol. Sci.* *146*, 439–459.
28. Chichery, M.P., and Chichery, R. (1987). The anterior basal lobe and control of prey-capture in the cuttlefish (*Sepia officinalis*). *Physiol. Behav.* *40*, 329–336.
29. Fiorito, G., and Chichery, R. (1995). Lesions of the vertical lobe impair visual discrimination learning by observation in *Octopus vulgaris*. *Neurosci. Lett.* *192*, 117–120.
30. Messenger, J.B. (1967). The effects on locomotion of lesions to the visuomotor system in octopus. *Proc. R. Soc. Lond. B Biol. Sci.* *167*, 252–281.
31. Graindorge, N., Alves, C., Darmaillacq, A.S., Chichery, R., Dickel, L., and Bellanger, C. (2006). Effects of dorsal and ventral vertical lobe electrolytic lesions on spatial learning and locomotor activity in *Sepia officinalis*. *Behav. Neurosci.* *120*, 1151–1158.
32. Miyan, J.A., and Messenger, J.B. (1995). Intracellular recordings from the chromatophore lobes of octopus. *Cephalopod Neurobiology* (Oxford University Press), pp. 415–429.
33. Chrachri, A., and Williamson, R. (2003). Modulation of spontaneous and evoked EPSCs and IPSCs in optic lobe neurons of cuttlefish *Sepia officinalis* by the neuropeptide FMRF-amide. *Eur. J. Neurosci.* *17*, 526–536.
34. Liu, T.H., and Chiao, C.C. (2017). Mosaic organization of body pattern control in the optic lobe of squids. *J. Neurosci.* *37*, 768–780.
35. Hu, M.Y., Yan, H.Y., Chung, W.S., Shiao, J.C., and Hwang, P.P. (2009). Acoustically evoked potentials in two cephalopods inferred using the auditory brainstem response (ABR) approach. *Comp. Biochem. Physiol. Mol. Integr. Physiol.* *153*, 278–283.
36. Chichery, R., and Chanelet, J. (1978). Motor responses obtained by stimulation of the peduncle lobe of *Sepia officinalis* in chronic experiments. *Brain Res.* *150*, 188–193.
37. Chichery, R., and Chanelet, J. (1976). Motor and behavioral responses obtained by stimulation with chronic electrodes of the optic lobe of *Sepia officinalis*. *Brain Res.* *105*, 525–532.
38. Dubas, F., Hanlon, R.T., Ferguson, G.P., and Pinsker, H.M. (1986). Localization and stimulation of chromatophore motoneurons in the brain of the squid, *Lolliguncula brevis*. *J. Exp. Biol.* *121*, 1–25.



39. Bullock, T.H., and Budelmann, B.U. (1991). Sensory evoked potentials in unanesthetized unrestrained cuttlefish: a new preparation for brain physiology in cephalopods. *J. Comp. Physiol.* **168**, 141–150.
40. Zullo, L., Sumbre, G., Agnisola, C., Flash, T., and Hochner, B. (2009). Nonsomatotopic organization of the higher motor centers in octopus. *Curr. Biol.* **19**, 1632–1636.
41. Hochner, B., Brown, E.R., Langella, M., Shomrat, T., and Fiorito, G. (2003). A learning and memory area in the octopus brain manifests a vertebrate-like long-term potentiation. *J. Neurophysiol.* **90**, 3547–3554.
42. Shomrat, T., Graindorge, N., Bellanger, C., Fiorito, G., Loewenstein, Y., and Hochner, B. (2011). Alternative sites of synaptic plasticity in two homologous “fan-out fan-in” learning and memory networks. *Curr. Biol.* **21**, 1773–1782.
43. Chung, W.S., López-Galán, A., Kurniawan, N.D., and Marshall, N.J. (2022). The brain structure and the neural network features of the diurnal cuttlefish *Sepia plangon*. *iScience*, 105846.
44. Young, J.Z. (1991). Computation in the learning system of cephalopods. *Biol. Bull.* **180**, 200–208.
45. Boycott, B.B., and Young, J.Z. (1955). A memory system in *Octopus vulgaris* Lamarck. *Proc. R. Soc. Lond. B Biol. Sci.* **143**, 449–480.
46. Shomrat, T., Zarrella, I., Fiorito, G., and Hochner, B. (2008). The octopus vertical lobe modulates short-term learning rate and uses LTP to acquire long-term memory. *Curr. Biol.* **18**, 337–342.
47. Sanders, F.K., and Young, J.Z. (1940). Learning and other functions of the higher nervous centres of *Sepia*. *J. Neurophysiol.* **3**, 501–526.
48. Jozet-Alves, C., Bertin, M., and Clayton, N.S. (2013). Evidence of episodic-like memory in cuttlefish. *Curr. Biol.* **23**, R1033–R1035.
49. Gutnick, T., Neef, A., Cherninsky, A., Ziadi-Künzli, F., Di Cosmo, A., Lipp, H.P., and Kuba, M.J. (2023). Recording electrical activity from the brain of behaving octopus. *Curr. Biol.* **33**, 1171–1178.e4.
50. Ramón y Cajal, S. (1930). Contribución Al Conocimiento De La Retina Y Centros Ópticos De Los Cefalópodos (Unión Internacional de Ciencias Biológicas, Comité Español).
51. Young, J.Z. (1960). The visual system of octopus: regularities in the retina and optic lobes of octopus in relation to form discrimination. *Nature* **186**, 836–839.
52. Liu, Y.C., Liu, T.H., Su, C.H., and Chiao, C.C. (2017). Neural organization of the optic lobe changes steadily from late embryonic stage to adulthood in cuttlefish *Sepia pharaonis*. *Front. Physiol.* **8**, 538.
53. Pungor, J.R., Allen, V.A., Songco-Casey, J.O., and Niell, C.M. (2023). Functional organization of visual responses in the octopus optic lobe. Preprint at bioRxiv. <https://doi.org/10.1101/2023.02.16.528734>.
54. Sereni, E., and Young, J.Z. (1932). Nervous degeneration and regeneration in cephalopods. *Pubbl. Staz. Zool. Napoli.* **12**, 173–208.
55. Gonzalez-Bellido, P.T., Scaros, A.T., Hanlon, R.T., and Wardill, T.J. (2018). Neural control of dynamic 3-dimensional skin papillae for cuttlefish camouflage. *iScience* **2**, 24–34.
56. Bühler, A., Froesch, D., Mangold, K., and Marthy, H.J. (1975). On the motor projection of the stellate ganglion in *Octopus vulgaris*. *Brain Res.* **88**, 69–72.
57. Wild, E., Wollesen, T., Haszprunar, G., and Heß, M. (2015). Comparative 3D microanatomy and histology of the eyes and central nervous systems in coleoid cephalopod hatchlings. *Org. Divers. Evol.* **15**, 37–64.
58. Hanlon, R.T., and Messenger, J.B. (1988). Adaptive coloration in young cuttlefish (*Sepia officinalis* L.): the morphology and development of body patterns and their relation to behaviour. *Philos. Trans. R. Soc. Lond. B Biol. Sci.* **320**, 437–487.
59. Duruz, J., Sprecher, M., Kaldun, J.C., Al-Soudy, A.S., Lischer, H.E.L., van Geest, G., Nicholson, P., Bruggmann, R., and Sprecher, S.G. (2023). Molecular characterization of cell types in the squid *Loligo vulgaris*. *eLife* **12**, e80670.
60. Songco-Casey, J.O., Coffing, G.C., Piscopo, D.M., Pungor, J.R., Kern, A.D., Miller, A.C., and Niell, C.M. (2022). Cell types and molecular architecture of the Octopus bimaculoides visual system. *Curr. Biol.* **32**, 5031–5044.e4.
61. Styfhals, R., Zolotarov, G., Hulselmans, G., Spanier, K.I., Poovathingal, S., Elagoz, A.M., De Winter, S., Deryckere, A., Rajewsky, N., Ponte, G., et al. (2022). Cell type diversity in a developing octopus brain. *Nat. Commun.* **13**, 7392.
62. Gavriouchkina, D., Tan, Y., Künzli-Ziadi, F., Hasegawa, Y., Piovani, L., Zhang, L., Sugimoto, C., Luscombe, N., Marlétaz, F., and Rokhsar, D.S. (2022). A single-cell atlas of bobtail squid visual and nervous system highlights molecular principles of convergent evolution. Preprint at bioRxiv. <https://doi.org/10.1101/2022.05.26.490366>.
63. dos Reis, M., Thawornwattana, Y., Angelis, K., Telford, M.J., Donoghue, P.C.J., and Yang, Z. (2015). Uncertainty in the timing of origin of animals and the limits of precision in molecular timescales. *Curr. Biol.* **25**, 2939–2950.
64. Shinomiya, K., Horne, J.A., McLin, S., Wiederman, M., Nern, A., Plaza, S.M., and Meinertzhagen, I.A. (2019). The organization of the second optic chiasm of the drosophila optic lobe. *Front. Neural Circuits* **13**, 65.
65. Gjerswold-Selleck, S., Zhu, N., Sun, H., Sikka, D., Shi, J., Liu, C., Nuriel, T., Small, S.A., and Guo, J. (2021). DL-BET-A deep learning based tool for automatic brain extraction from structural magnetic resonance images in mice. *Proc. Intl. Soc. Mag. Reson. Med.* **29**, 3486.
66. Fedorov, A., Beichel, R., Kalpathy-Cramer, J., Finet, J., Fillion-Robin, J.C., Pujol, S., Bauer, C., Jennings, D., Fennessy, F., Sonka, M., et al. (2012). 3D Slicer as an image computing platform for the Quantitative Imaging Network. *Magn. Reson. Imaging* **30**, 1323–1341.
67. Schindelin, J., Arganda-Carreras, I., Frise, E., Kaynig, V., Longair, M., Pietzsch, T., Preibisch, S., Rueden, C., Saalfeld, S., Schmid, B., et al. (2012). Fiji: an open-source platform for biological-image analysis. *Nat. Methods* **9**, 676–682.
68. Fiorito, G., Affuso, A., Basil, J., Cole, A., de Girolamo, P., D’Angelo, L., Dickel, L., Gestal, C., Grasso, F., Kuba, M., et al. (2015). Guidelines for the Care and Welfare of Cephalopods in Research -A consensus based on an initiative by CephRes, FELASA and the Boyd Group. *Lab. Anim.* **49**, 1–90.
69. Tustison, N.J., Avants, B.B., Cook, P.A., Zheng, Y., Egan, A., Yushkevich, P.A., and Gee, J.C. (2010). N4ITK: improved N3 bias correction. *IEEE Trans. Med. Imaging* **29**, 1310–1320.
70. Avants, B.B., Tustison, N.J., Song, G., Cook, P.A., Klein, A., and Gee, J.C. (2011). A reproducible evaluation of ANTs similarity metric performance in brain image registration. *Neuroimage* **54**, 2033–2044.
71. Gestal, C., Pascual, S., Guerra, Á., Fiorito, G., and Vieites, J.M. (2019). *Handbook of Pathogens and Diseases in Cephalopods* (Springer).

## STAR★METHODS

### KEY RESOURCES TABLE

REAGENT or RESOURCE	SOURCE	IDENTIFIER
<b>Biological samples</b>		
<i>Sepia bandensis</i> (dwarf cuttlefish)	Quality Marine	N/A
<b>Chemicals, peptides, and recombinant proteins</b>		
Marinemix salt	Crystal Sea	N/A
Paraformaldehyde (16%)	Electron Microscopy Services	15710
Omniscan (gadodiamide)	GE Healthcare	0407-0690-10
Fomblin	Thermo Scientific Chemicals	L17548.14
Tissue-Tek O.C.T. compound	Sakura Finetek	25608-930
Alexa Fluor 488 Phalloidin	Life Technologies	A12379
NeuroTrace 520/615 Red Fluorescent Nissl Stain	Invitrogen	N21482
<b>Deposited data</b>		
Cuttlefish MRI and histology brain data	This paper	<a href="https://www.cuttlebase.org/downloads">https://www.cuttlebase.org/downloads</a>
Cuttlefish 3D brain and body models	This paper	<a href="https://www.cuttlebase.org/downloads">https://www.cuttlebase.org/downloads</a>
<b>Software and algorithms</b>		
DL-BET	Gjerswold-Selleck et al. <sup>65</sup>	<a href="https://github.com/SAIL-GuoLab/DL-BET">https://github.com/SAIL-GuoLab/DL-BET</a>
Cuttlebase template brain generation	This paper	<a href="https://github.com/SAIL-GuoLab/Cuttlebase">https://github.com/SAIL-GuoLab/Cuttlebase</a>
Cuttlebase image processing utility scripts	This paper	<a href="https://github.com/noisyneuron/cuttlebase-util">https://github.com/noisyneuron/cuttlebase-util</a>
Cuttlebase web content delivery	This paper	<a href="https://github.com/noisyneuron/cuttlebase-website">https://github.com/noisyneuron/cuttlebase-website</a>
3D Slicer	Fedorov et al. <sup>66</sup>	<a href="https://www.slicer.org/">https://www.slicer.org/</a>
BrainJ	This paper	<a href="https://github.com/lahammond/BrainJ">https://github.com/lahammond/BrainJ</a>
Fiji	Schindelin et al. <sup>67</sup>	<a href="https://fiji.sc/">https://fiji.sc/</a>

### RESOURCE AVAILABILITY

#### Lead contact

Further information and requests for resources and reagents should be directed to and will be fulfilled by the lead contact, Tessa Montague ([tessa.montague@columbia.edu](mailto:tessa.montague@columbia.edu)).

#### Materials availability

This study did not generate new unique reagents.

#### Data and code availability

The MRI data, histology data, 3D brain and 3D body models have been deposited on Cuttlebase and are publicly available (for links see [key resources table](#)). All original code has been deposited at GitHub (see [key resources table](#)). Any additional information required to reanalyze the data reported in this paper is available from the lead contact upon request.

### EXPERIMENTAL MODEL AND SUBJECT DETAILS

#### Ethics statement

The use of cephalopods in laboratory research is currently not regulated in the USA. However, Columbia University has established strict policies for the ethical use of cephalopods, including operational oversight from the Institutional Animal Care and Use Committee (IACUC). All of the cuttlefish used in this study were handled according to an approved IACUC protocol (AC-AABE3564), including the use of deep anesthesia and the minimization and prevention of suffering. The animal handling also adhered to European Directive 2010/63/EU.<sup>68</sup>

#### Cuttlefish husbandry

Dwarf cuttlefish (*Sepia bandensis*) were housed in 10-gallon glass tanks in groups (<4 adults) within a recirculating 250-gallon system of 32 parts per thousand (ppt) artificial seawater (Crystal Sea Marinemix) maintained at 76°F. Adult cuttlefish were fed 3 live grass

shrimp (*Palaemonetes pugio*, Aquatic Indicators), 3 times per day. Frequent water changes and mechanical, chemical and biological filtration were used to maintain water quality parameters: ammonia 0 parts per million (ppm), nitrite <0.1 ppm, nitrate <20 ppm and pH 8.1–8.4.

## METHOD DETAILS

### 3D brain atlas

#### MRI acquisition

8 adult cuttlefish (4 male, 4 female; 6–7 months old; average mantle length 60 mm) were anesthetized in a solution of 1% ethanol/artificial seawater and then euthanized in 10% ethanol for 10 min followed by decapitation. The brains and connected eyes were surgically removed and fixed overnight in a solution of 4% paraformaldehyde (PFA) in filtered artificial seawater (FASW) at 4°C. The fixed brains were washed in PBS, incubated in 0.2% Omniscan (gadodiamide) for 2 days at 4°C to increase contrast, and then suspended in fomblin in a 15 mL conical tube. Imaging was performed on a Bruker BioSpec 94/30 horizontal small animal MRI scanner (field strength, 9.4 T; bore size, 30 cm) equipped with a CryoProbe and ParaVision 6.0.1 software (Bruker). A 23 mm 1H circularly polarized transmit/receive-capable mouse head volume coil was used for imaging. For each cuttlefish, one scan was acquired of the brain and eyes (to obtain a scan of the entire cranial cartilage), and a higher resolution scan was acquired of the brain only. T1-weighted images were acquired with a Fast Low Angle Shot (FLASH) sequence (brain/eye scan: TR = 50 ms, TE = 10 ms, FOV = 30 × 24 × 15 mm<sup>3</sup>, voxel size = 100 × 100 × 100 μm<sup>3</sup>, scan time = 33 m 12 s; brain-only scan: TR = 50 ms, TE = 8.5 ms, FOV = 14 × 12 × 11 mm<sup>3</sup>, voxel size = 60 × 60 × 60 μm<sup>3</sup>, scan time = 4 hr 28 m).

#### MRI processing & brain extraction

All scans underwent N4 bias field correction.<sup>69</sup> Whole brain scans were isotropically upsampled to 50 μm isotropic resolution with cubic B-spline interpolation. To computationally extract the brains from their surrounding tissue, brain masks were generated by an in-house deep learning model,<sup>65</sup> which was pre-trained with brain masks manually annotated in 3D Slicer.<sup>66</sup> The deep learning brain masks were manually polished using the 3D Slicer Segment Editor and then used to extract the brain from each brain-only MRI scan (“brain-extracted images”) (Figure S1). For the brain/eye scans, the cranial cartilage was manually segmented in 3D Slicer using the Segment Editor. The cartilage masks were used to extract the cartilage from each brain/eye MRI scan (“cartilage-extracted images”).

#### Segmentation

Two of the whole brain scans (1 male, 1 female) were manually segmented in 3D Slicer by 6 independent annotators guided by prior neuroanatomical descriptions.<sup>18,19</sup> The brain label maps for each subject were merged using pixel-level majority voting, transformed to the remaining 6 subjects, and then manually corrected, resulting in 8 brain label maps corresponding to the 8 subjects. Lobe locations were determined by prior annotations<sup>18,19</sup> and precise lobe boundaries were estimated using the location of an outer cell body layer, which is a feature of most cephalopod brain lobes. The combined use of high-resolution histological data and three-dimensional MRI data aided the discrimination of lobes in 3D space.

#### Generation of the template brain

The final MRI atlas was built by merging the brain template, built from the high-resolution brain-only scans and their mirror images, with the cranial cartilage template, built from the brain/eye scans. First, to generate each template, a population average of brain-extracted or cartilage-extracted images was constructed through an iterative process by averaging the co-registered images over multiple cycles using a symmetric diffeomorphic registration algorithm.<sup>70</sup> The brain label map (annotations) for each subject was diffeomorphically transformed to the whole brain template space and combined through pixel-level majority voting. The brain/eye template was isotropically upsampled to match the 50 μm resolution of the whole brain scans, and the whole brain template underwent rigid registration to align it with the brain/eye template. Finally, the brain regions of the whole brain template were combined with the cartilage regions of the whole head template to build a single atlas. In the regions where the two templates overlapped, pixel values of the high-resolution whole brain template were selected. The cuttlefish brain label map was smoothed by taking a majority vote in a local neighborhood with a 3 × 3 × 3 kernel size.

#### Brain volume calculations

A mouse MRI brain model (15 μm resolution, average of 18 *ex vivo* subjects) was downloaded from the Australian Mouse Brain Mapping Consortium (nonsymmetric version, NiftI format, <https://imaging.org.au/AMBMC/Model>), and then downsampled to 50 μm resolution and imported into 3D Slicer. Using the Editor tool at a threshold of zero, a mask was generated of the entire mouse brain, and the spinal cord was manually removed using the eraser tool. The volume of the mouse brain mask was calculated using the Label Statistics tool (total volume: 332.7 mm<sup>3</sup>). Cuttlefish brain lobe volumes were calculated using the Label Statistics tool in 3D Slicer (see Tables S1–S4). The total cuttlefish template brain volume was calculated by summing the volumes of all internal brain lobes and nerves (total volume: 312.1 mm<sup>3</sup>).

#### Histological atlas

Adult cuttlefish were anesthetized in a solution of 1% ethanol/artificial seawater and then euthanized in 10% ethanol for 10 min followed by decapitation. The brains and connected eyes were surgically removed and fixed overnight in a solution of 4% paraformaldehyde (PFA) in filtered artificial seawater (FASW) at 4°C. Note that fixing brains in a solution of PBS (instead of FASW) created abnormal cell morphologies. The fixed brains were washed in PBS, the eyes were removed with a scalpel, and the brains were

incubated in 10% sucrose overnight followed by 30% sucrose overnight at 4°C. The brains were embedded in O.C.T. on dry ice and stored at -80°C. Each brain was sliced in 100 μm sections on a cryostat (Leica CM3050 S), and the sections were dried overnight at room temperature. The sections were stained with Phalloidin (Life Technologies #A12379, 1/40 dilution) and NeuroTrace (Life Technologies #N21482, 1/20 dilution) and then imaged on a custom-built Nikon AZ100 Multizoom Slide Scanner. Images were registered using BrainJ (<http://github.com/lahammond/BrainJ>). Brightness and contrast were adjusted uniformly across each image, and surrounding tissue was removed manually from the image in Fiji<sup>67</sup> and Photoshop. The data was manually segmented in 3D Slicer by two annotators using a neuroanatomical study<sup>18</sup> and our 3D brain data for reference.

### Whole body atlas

An adult male cuttlefish was anesthetized in MgCl<sub>2</sub> (17.5 g/L) and then euthanized in 10% ethanol, fixed for 2 days in 4% PFA/FASW at 4°C, and then incubated in 0.2% Omniscan (gadodiamide) for 2 days at 4°C to increase contrast. The fixed specimen was suspended in fomblin in a custom-made vessel and imaged on a Bruker BioSpec 94/30 horizontal small animal MRI scanner (field strength, 9.4 T; bore size, 30 cm) equipped with a CryoProbe and ParaVision 6.0.1 software (Bruker). A 112/86-mm 1H circularly polarized transmit/receive-capable volume coil was used for imaging. T1-weighted images were acquired with a FLASH sequence (TR = 55 ms, TE = 17 ms, FOV = 90 × 48 × 38 mm<sup>3</sup>, voxel size = 100 × 100 × 100 μm<sup>3</sup>, scan time = 2 hr 47 m). The scan underwent N4 bias field correction<sup>69</sup> and was manually segmented in 3D Slicer using anatomical descriptions.<sup>71</sup>

### Cuttlebase

The Cuttlebase web content is delivered using React, a JavaScript front-end framework for dynamic websites. React-three-fiber (a Three.js wrapper for React) is used to assist with interactions in the 3D view.

#### 3D brain

In 3D Slicer, each segment (brain lobe or tract) of the final, template brain was exported as an STL file and then labelled with a unique identifier in Blender, a 3D authoring software. The 3D model was exported as a GLB, and then imported into a webpage using Three.js - a JavaScript library for handling 3D content on the web. A custom web-interface was created to assign colors to each of the region meshes, and this data was exported as a JSON file.

#### Histology

To convert the histological annotations to high-resolution images that could be toggled on Cuttlebase, each segment (brain lobe or tract) for each brain (horizontal, sagittal and transverse) was converted to a binary label map in 3D Slicer and saved as a TIFF stack. Each TIFF stack was resized to the canvas size of the original image in Fiji,<sup>67</sup> and saved as a JPEG stack in monochrome. The images were then inverted and processed with Potrace (through a custom Node.js script), to create SVGs for each region of each layer. The SVGs for all regions in a single layer were combined, and each region was assigned the color corresponding to the 3D atlas. These images, along with the originals, were resized and cropped for more efficient web delivery. Additionally, the cartilage in each Phalloidin section was isolated (by outlining) using Adobe Illustrator, and exported as a PNG. These images were used as masks on the NeuroTrace layers with the command-line tool ImageMagick, to automate this process for the remaining images. Custom Bash scripts were used to manage and organize the large amounts of data and the processing steps required.

### QUANTIFICATION AND STATISTICAL ANALYSIS

Brain lobe volumes were calculated in 3D Slicer using the Label Statistics tool. For each brain lobe, the standard deviation (SD) of lobe volumes was calculated across the 8 brains (see [Tables S1](#) and [S2](#)). T-tests comparing lobe volumes in the 4 female and 4 male brains were calculated using a two-tailed distribution and two-sample equal variance test (see [Tables S1](#) and [S2](#)).